

A Program to Estimate Resolution for Charged Particles in GlueX

GlueX-doc-1015-v2

Mark M. Ito
Thomas Jefferson National Accelerator Facility
12000 Jefferson Avenue
Newport News, VA 23606

April 15, 2008

Abstract

This note describes a set of FORTRAN routines (**REZEST**) that estimates charged track resolution in transverse momentum and direction for the GlueX detector geometry. Parameters of that geometry can be varied to quickly obtain estimates for new configurations. Since no Monte Carlo is used in the calculations, results are returned immediately. Instructions on how to obtain and use the software are provided and a description of the approximations used is given.

Contents

1	Introduction	2
2	Using the Software	3
2.1	Getting the code	3
2.2	Building the files	3
2.3	Using the files	4
2.3.1	<code>librezest.a</code>	4
2.3.2	<code>rezest_point</code>	4
2.3.3	<code>rezest_point_comp</code>	4
3	How the Estimates Are Done	5
3.1	Transverse Momentum Resolution	6
3.2	Curvature vs. Momentum	6
3.3	Error on Slope and y -intercept of a Straight-Line Fit, Equally Spaced Measurements	6
3.4	Angular Error Due to Multiple Coulomb Scattering	7
3.5	Contribution to Azimuthal Angle Resolution from Curvature Resolution	8
3.6	Geometry of the CDC	10
3.7	Geometry of the FDC	10
3.8	Combining the CDC and the FDC	12
4	Results	12
5	Conclusions	12
A	Some useful equations	12

1 Introduction

We often use “back of the envelope” estimates of detector performance to inform detailed design decisions. These calculations have the advantage of simplicity and provide quick feedback for new design ideas. The FORTRAN routines described here provide a facility for making such calculations for GlueX.

The fixed detector geometry concept used is the standard one for GlueX: a central cylindrical drift chamber (CDC) in a solenoidal field with a set of planar drift chambers in the forward direction (FDC). The CDC is assumed to have both axial and stereo layers. The parameters that can be varied include:

- z position¹ of the target
- inner and outer radius of the CDC
- length of the CDC
- front and back z -positions of the FDC
- amount of material in the FDC and CDC tracking volume
- amount of material in front of the FDC and CDC
- magnetic field strength
- number of axial and stereo position measurements in the CDC
- stereo angle for stereo layers in the CDC
- number of position measurements in the FDC

Many approximations are made and generic formulae applied in the calculations. The numbers that are produced are not a substitute for a full-scale, hit-based Monte Carlo simulation of the detector. That having been said, the relative variation of resolution when a particular parameters are varied should give a good feeling for the effect of parameter change.

The following assumptions are made:

- The magnetic field is uniform everywhere.
- Particles travel in straight lines, independent of momentum.²
- Measurements of track parameters in the FDC are statistically independent from those made in the CDC.
- All position measurements within a detector (FDC or CDC) are statistical independent of one another.
- All positions measurements within a detector are made at locations uniformly spaced along the trajectory.
- All positions measurements within a detector have the same resolution.

A note on notation: in the following, σ_x and δx will be used interchangeable to represent the root mean square deviation of the quantity x .

¹The z -direction is along the incident photon beam.

²Of course, charged particles must curve in the magnetic field to make a momentum measurement possible. This assumption is only relevant in determining where a particle went; *i. e.*, what parts of the detectors it crossed and how much material it encountered.

2 Using the Software

The principal subroutine is documented in the source code file `rezest_fdc_cdc.F`:

```
      SUBROUTINE REZEST_FDC_CDC(P, LAMBDA, M,
      X      DP_OVER_P, DPHI_TOT, DTHETA_TOT)
CCCCCCCCCCCCCCCCCCCCCCCCCCCCCCCCCCCCCCCCCCCCCCCCCCCCCCCCCCCC
C
C This routine estimates the resolution in GlueX for charged particles
C in tranverse momentum, azimuthal angle, and polar angle.
C
C Input arguments, all REAL*4
C
C   P      Magnitude of total momentum (GeV/c)
C   LAMBDA  Dip angle, difference in polar angle in lab between track
C           and pi/2 (i. e., 90 degrees) (radians)
C   M      Mass of the particle (GeV/c^2)
C
C Output arguments, all REAL*4
C
C   DP_OVER_P  Relative resolution in transverse momentum
C              ("sigma_{p_t}/p_t")
C   DPHI_TOT   Resolution in azimuthal angle ("sigma_phi")
C   DTHETA_TOT Resolution in polar angle ("sigma_theta")
C
C The routine combines the measurements in the FDC and CDC where
C appropriate. Parameters describing the geometry and materials are
C defined in the routine REZEST_COMPONENTS which appears below.
C
```

2.1 Getting the code

Two methods:

1. Get the tar ball from

<http://www.jlab.org/~marki/misc/rezest.tar>

2. Check it out from the subversion repository with the command

```
svn checkout https://halldsvn.jlab.org/repos/trunk/home/marki/glueX/rezest
```

2.2 Building the files

There is a simple makefile in the directory:

```
> cd <rezest directory>
> make
gfortran -g -c -o rezest.o rezest.F
gfortran -g -c -o rezest_fdc_cdc.o rezest_fdc_cdc.F
ar rcv librezest.a rezest.o rezest_fdc_cdc.o
a - rezest.o
a - rezest_fdc_cdc.o
gfortran -g -c -o rezest_point.o rezest_point.F
gfortran -o rezest_point rezest_point.o -L. -lrezest
gfortran -g -c -o rezest_point_comp.o rezest_point_comp.F
gfortran -o rezest_point_comp rezest_point_comp.o -L. -lrezest
```

This creates three files that you care about:

1. `librezest.a`: the object library
2. `rezest_point`: a binary
3. `rezest_point_comp`: a binary

2.3 Using the files

2.3.1 `librezest.a`

Link this into your own program to retrieve resolution values. It contains the routine `rezest_fdc_cdc` described in Section 2.

2.3.2 `rezest_point`

This stand-alone binary will accept three arguments on standard input (space separated on a single line) and will write the resolution values on standard output.

Input:

1. total magnitude of momentum in GeV/c
2. dip angle in radians (polar angle referenced from 90° in the lab; $\theta_{\text{dip}} = \pi/2 - \theta$ there θ is the standard polar angle)
3. mass in GeV/c²

Output:

1. relative resolution in transverse momentum ($\delta p_t/p_t$)
2. resolution in azimuthal angle ($\delta\phi$)
3. resolution in polar angle ($\delta\theta$)

For example:

```
> rezest_point
1.0 1.22 0.139
 2.8597742E-02  1.6185496E-02  8.1181811E-04
```

says that a 1 GeV/c particle traveling in a direction 1.22 radians forward of the transverse direction with a mass of 139 MeV has an estimated $\delta p_t/p_t = 2.9\%$, $\delta\phi = 16$ mrad, and $\delta\theta = 0.8$ mrad.

2.3.3 `rezest_point_comp`

Same as `rezest_point` except that the individual components of the resolution are listed. Note that the first three numbers being output are the same as for `rezest_point`.

Output:

1. relative resolution in transverse momentum
2. resolution in azimuthal angle
3. resolution in polar angle
4. resolution in curvature ($k = 1/R$) due to multiple scattering in the CDC in inverse meters
5. same for FDC
6. resolution in curvature due to position resolution in the CDC

7. same for FDC
8. total resolution in curvature in the CDC
9. same for the FDC
10. resolution in azimuthal angle (ϕ) due to multiple scattering in the CDC in radians
11. same for FDC
12. resolution in azimuthal angle due to position resolution in the CDC
13. same for FDC
14. resolution in azimuthal angle due to curvature resolution in the CDC
15. same for FDC
16. total resolution in azimuthal angle in the CDC
17. same for the FDC
18. resolution in polar angle (θ) due to multiple scattering in the CDC in radians
19. same for FDC
20. resolution in polar angle due to position resolution in the CDC in radians
21. same for FDC
22. total resolution in polar angle in the CDC
23. same for the FDC

For example:

```
> rezest_point_comp
1.0 1.22 0.139
 2.8597742E-02  1.6185496E-02  8.1181811E-04  4.2887099E-02
 2.2642065E-02  1.3919008E-02  0.1605156      4.5089267E-02
 0.1621047      2.5197803E-03  3.1950074E-04  5.0111138E-04
 2.4516270E-03  1.7020071E-02  4.7496673E-02  1.7212879E-02
 4.7560975E-02  2.5197803E-03  3.1950074E-04  7.7741774E-04
 7.9118297E-04  2.6369814E-03  8.5325917E-04
```

(All values in the output actually appear on one line.)

3 How the Estimates Are Done

In this section the various formulae and concepts used to produce the estimates are described.

3.1 Transverse Momentum Resolution

The formulae used to estimate transverse are taken from the Particle Data Group's Review of Particle Physics[2]. Using (for the most part) their notation and descriptions, for a particle with charge q of momentum p in a uniform magnetic field B with a pitch³ angle λ

$$p_t \equiv p \cos \lambda = (0.3)qBR \quad (1)$$

where R is the radius of curvature in the projection of the trajectory onto the bend plane, p is in GeV/c, B is in Tesla, and R is in meters. In the remainder of this note it will be assumed that $q = 1$. Further, the magnetic field is assumed to be uniform everywhere and in the z -direction. The curvature $k = \frac{1}{R}$. The variance of k has two contributions,

$$(\delta k)^2 = (\delta k_{\text{res}})^2 + (\delta k_{\text{ms}})^2. \quad (2)$$

$$\delta k_{\text{res}} = \frac{\epsilon}{L'^2} \sqrt{\frac{720}{N+4}} \quad (3)$$

where ϵ is the position resolution in meters, L' is the projected length of the track onto the bending plane in meters and N is the number of measurements.

$$\delta k_{\text{ms}} = \frac{(0.016 \text{ GeV}/c)z}{Lp\beta \cos^2 \lambda} \sqrt{n_{\text{RL}}} \quad (4)$$

where n_{RL} is the number of radiation lengths in the detector and L is the total track length in the detector. For the momentum estimate, the amount of material in front of the detector is ignored.

3.2 Curvature vs. Momentum

The estimates in the previous section are given in terms of the error on curvature. These must be converted to momentum. Rewriting Eq. 1

$$p_t = (0.3)BR = \frac{(0.3)B}{k} \quad (5)$$

So

$$\frac{dp_t}{dk} = -\frac{(0.3)B}{k^2} = -(0.3)BR^2 \quad (6)$$

and since

$$\delta p_t = \left| \frac{dp_t}{dk} \right| \delta k, \quad (7)$$

we have

$$\frac{\delta p_t}{p_t} = R\delta k = \frac{\delta k}{k}. \quad (8)$$

3.3 Error on Slope and y -intercept of a Straight-Line Fit, Equally Spaced Measurements

To estimate the error due to position resolution on the direction of a fitted track, we use the error on the slope of a straight line fitted to the same number of measurements as the fundamental input. This approach ignores the fact that the trajectory is in fact curved, but is being used to estimate the error in the angle and not the angle itself.

From Ref. [1]

$$\chi^2 = \sum \left[\frac{1}{\sigma_i^2} (y_i - a - bx_i)^2 \right] \quad (9)$$

³ λ is sometimes called the dip angle. It is the angle of the trajectory with respect to a plane transverse to the magnetic field. Note that a trajectory with a polar angle of 90° has a pitch angle of 0.

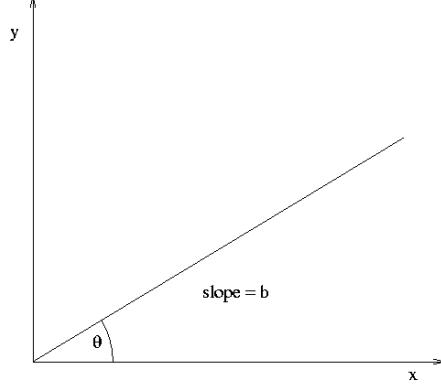


Figure 1: Generic straight line through origin.

For equal errors ($\sigma_i = \sigma \forall i$), χ^2 is minimized for a and b when

$$a = \frac{1}{\Delta'} \left(\sum x_i^2 \sum y_i - \sum x_i \sum x_i y_i \right) \quad (10)$$

$$b = \frac{1}{\Delta'} \left(n \sum x_i y_i - \sum x_i \sum y_i \right) \quad (11)$$

where

$$\Delta' = n \sum x_i^2 - \left(\sum x_i \right)^2 \quad (12)$$

The variance of the parameters a and b are

$$\sigma_a^2 \approx \frac{\sigma^2}{\Delta'} \sum x_i^2 \quad (13)$$

and

$$\sigma_b^2 \approx \frac{n\sigma^2}{\Delta'}. \quad (14)$$

For n equally spaced measurements spanning the interval $[0, L]$,

$$x_i = \frac{L(i-1)}{n-1} \quad (15)$$

and using expressions from Appendix A, we get

$$\sigma_a^2 = \frac{2\sigma^2(2n-1)}{n(n+1)} \quad (16)$$

$$\sigma_b^2 = \frac{12\sigma^2(n-1)}{L^2 n(n+1)} \quad (17)$$

We need to translate an error in slope to an error in angle. In Fig. 1, $\theta = \tan^{-1} b$ so

$$\delta\theta = \left| \frac{d\theta}{db} \right| \delta b = \frac{\delta b}{\sec^2 \theta}. \quad (18)$$

3.4 Angular Error Due to Multiple Coulomb Scattering

Again from Ref. [2], we define

$$\theta_0 = \theta_{\text{plane}}^{\text{rms}} = \frac{1}{\sqrt{2}} \theta_{\text{space}}^{\text{rms}}. \quad (19)$$

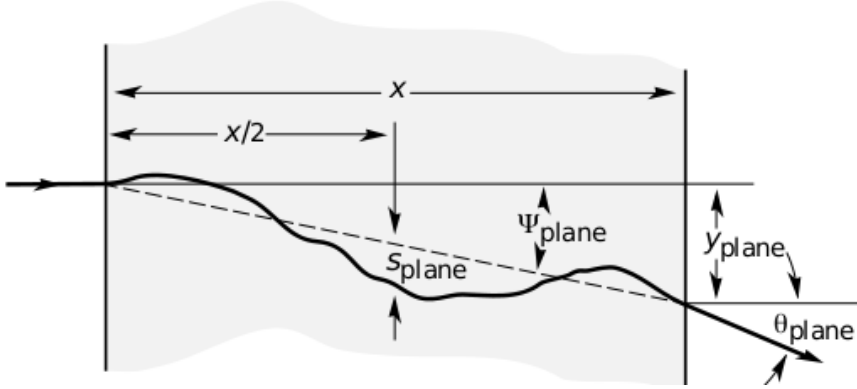


Figure 2: Quantities used to describe multiple Coulomb scattering. The particle is incident in the plane of the figure.

The central angular distribution is approximately Gaussian with a width given by

$$\theta_0 = \frac{(13.6 \text{ MeV})}{\beta c p} z \sqrt{x/X_0} [1 + 0.038 \ln(x/X_0)]. \quad (20)$$

As seen in Fig. 2, the angle Ψ_{plane} is the angle between an unscattered trajectory and a line drawn from the entrance point of the detector to the exit point. We use this as an approximation to the contribution of multiple scattering to both the azimuthal and polar angles.

$$\Psi_{\text{plane}}^{\text{rms}} = \frac{1}{\sqrt{3}} \theta_0. \quad (21)$$

When estimating angular resolution, the material in front of a particular detector (“fronting material”) is included as an addition to the number of radiation lengths in the detector itself.

If two detectors are traversed by a particle the material in front of the first detector and the material in the first detector itself are ignored, since the resolution of both will be combined at a later stage (see Section 3.8).

3.5 Contribution to Azimuthal Angle Resolution from Curvature Resolution

The curvature $k = 1/R$ and direction in the bending plane is measured at a “point” (actually a region in the plane) rotated from the vertex by an angle α about the center of curvature, not at the vertex. To infer the azimuthal angle ϕ at the vertex, track must be swum backward through angle α . Determination of α depends on R and thus on k . An error in α translates directly into an error in ϕ .

$$\sin \frac{\alpha}{2} = \frac{r_{\text{mid}}}{2R} = \frac{r_{\text{mid}} k}{2} \quad (22)$$

so

$$\delta\alpha = r_{\text{mid}} \delta k \sec \frac{\alpha}{2} \quad (23)$$

where $\alpha = 2 \sin^{-1}(r_{\text{mid}}/2R)$. As an approximation, we take $r_{\text{mid}} = (r_{\text{in}} + r_{\text{out}})/2$.

Note that a side effect of using a straight-line approximation for the trajectory is that in some cases r_{out} can be greater than $2R$, *i. e.*, the curving track never reaches the outer radius obtained from the straight-line approximation. In those cases, the outer radius is set to $2R$. This avoids arguments to the inverse sine greater than one.

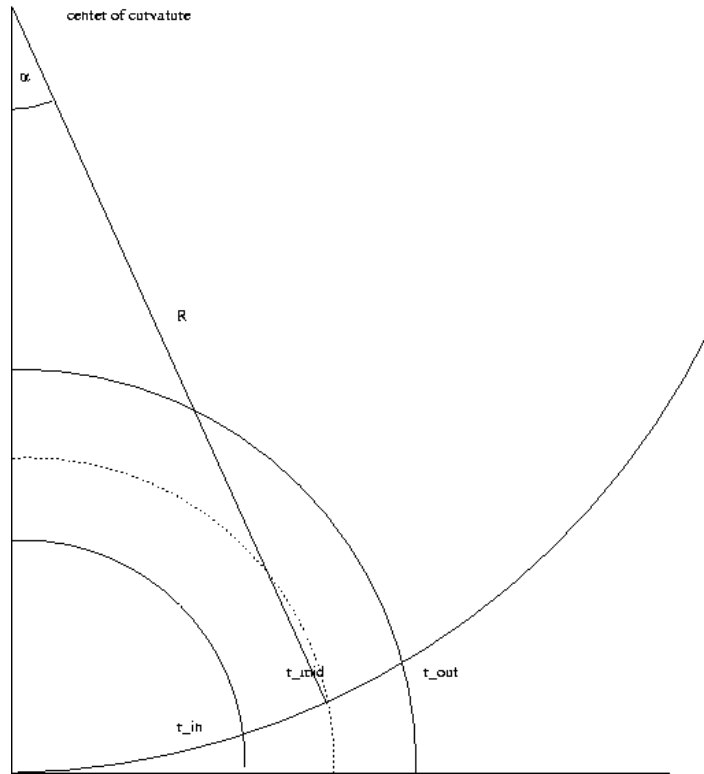


Figure 3: The concept for estimating the effect of curvature resolution on azimuthal angle resolution.

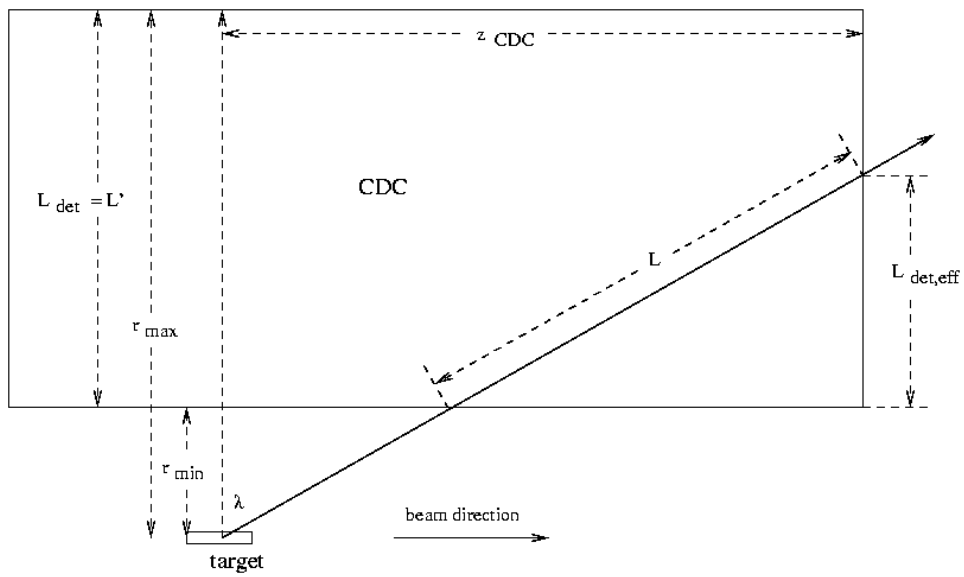


Figure 4: Geometry of the CDC

Parameter	Value
r_{\min}	0.10960 m
r_{\max}	0.56534 m
z_{CDC}	1.02 m
$r_{\min,\text{stereo}}$	0.16304 m
$r_{\max,\text{stereo}}$	0.39473 m
$n_{\text{RL,CDC}}$	0.03437
$n_{\text{RL,front}}$	0.01437
$n_{\text{RL,endplate}}$	0.02810
$n_{\text{m,CDC}}$	25
$n_{\text{m,stereo}}$	8

Table 1: Values of geometry parameters for the CDC in the current design.

3.6 Geometry of the CDC

Fig. 4 shows a schematic of the CDC chamber displaying some of the parameters that serve as input to the estimate:

r_{\min} minimum radius of the CDC tracking volume

r_{\max} maximum radius of the CDC tracking volume

z_{CDC} z -coordinate distance from center of target to downstream end of the CDC

Other parameters, not shown in Fig. 4 are:

$r_{\min,\text{stereo}}$ minimum radius of the CDC stereo layers

$r_{\max,\text{stereo}}$ maximum radius of the CDC stereo layers

$n_{\text{RL,CDC}}$ number of radiation lengths measured transverse to the tracking layers, *i. e.*, at 90° in the lab ($n_{\text{rl}} = x/X_0$)

$n_{\text{RL,front}}$ number of radiation lengths in the material inside the CDC (target, scattering chamber, start counter, *etc.*), measured radially from the beam line.

$n_{\text{RL,endplate}}$ number of radiation lengths in the downstream CDC endplate, measured along the beam direction

$n_{\text{m,CDC}}$ number of position measurements for a track which passes through all layers of the CDC (sum of number of axial and stereo layers)

$n_{\text{m,stereo}}$ number of position measurements in stereo layers

Table 1 gives the values for these parameters in the current design.

For the CDC, $L_{\text{det}} = r_{\max,\text{CDC}} - r_{\min,\text{CDC}}$ is the radial thickness of the active volume. Then $L' = L_{\text{det}}$ and $L = L_{\text{det}} / \cos \lambda$.

For tracks that exit the end of the CDC, the straight-line track approximation is used to scale the number of measurements, the number of radiation lengths and the transverse length of the track (L'). Also for tracks exiting through the end-plate, the material in the endplate is used as the material in front of the FDC.

3.7 Geometry of the FDC

Fig. 5 shows a schematic of the FDC chamber displaying some of the parameters that serve as input to the estimate:

z_{\min} minimum z of the FDC tracking volume

z_{\max} maximum z of the FDC tracking volume

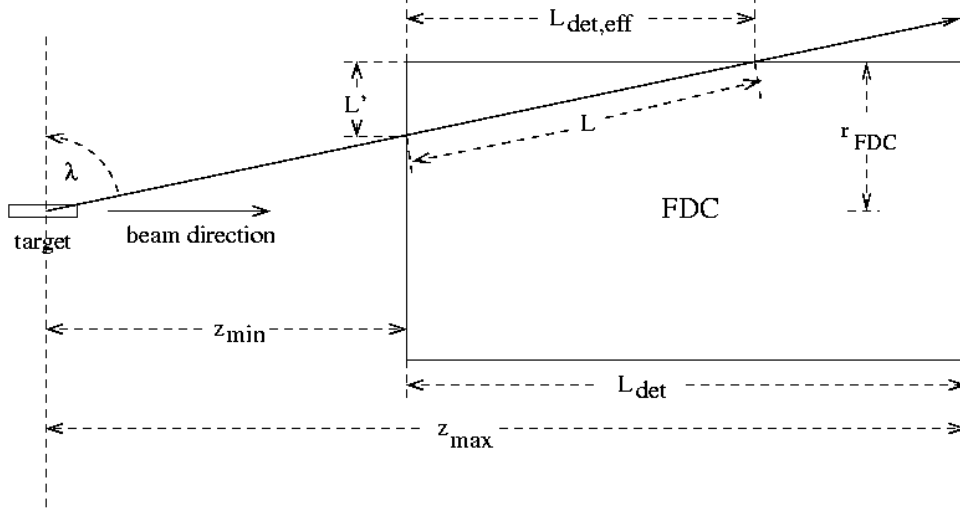


Figure 5: Geometry of the FDC.

Parameter	Value
z_{\min}	1.25 m
z_{\max}	2.92 m
r_{FDC}	0.56534 m
$n_{\text{RL,FDC}}$	0.028258
$n_{\text{m,FDC}}$	24

Table 2: Values of geometry parameters for the FDC in the current design.

r_{FDC} outer radius of the FDC

Other parameters, not shown in Fig. 5, are:

$n_{\text{RL,FDC}}$ number of radiation lengths measured transverse to the tracking layers, *i. e.*, in the forward direction ($n_{\text{rl}} = x/X_0$)

$n_{\text{m,FDC}}$ number of one-dimensional position measurements for a track which passes through all layers of the FDC⁴

Table 2 gives the values for these parameters in the current design.

For the FDC $L_{\text{det}} = z_{\max} - z_{\min}$ is the length of the active volume along the beam direction. Then $L' = L_{\text{det}} / \tan \lambda$ and $L = L_{\text{det}} / \sin \lambda$.

For tracks that exit the side of the FDC, like the CDC, the straight-line track approximation is used both to determine if the track is “exiting early” and to scale the number of measurements, the number of radiation lengths and the transverse length of the track (L').

The material used in front of the FDC for tracks which miss the CDC is that same as that used for the FDC to represent the target and other inner components. If the track passes through the end-plate of the CDC, then only the end-plate material is used as the fronting material (as mentioned in Section 3.6). In this case since the effect of the inner material is included in the estimate of angular resolution for the CDC, it should not be included in the resolution estimate for the FDC.

⁴Since not all layers of the FDC will yield position measurements in a particular chosen dimension, the number of effective measurement planes will be only a fraction of the total measurement planes present in the chamber. While this is true of the CDC as well, the stereo angle is assumed to be so small that stereo layers are assumed to contribute fully to position determination in the r - ϕ plane (an approximation).

3.8 Combining the CDC and the FDC

For each quantity, the measurements in the CDC and FDC are statistically independent. They are therefore combined using:

$$\sigma_{\text{total}} = \frac{1}{\sqrt{\frac{1}{\sigma_{\text{CDC}}^2} + \frac{1}{\sigma_{\text{FDC}}^2}}} \quad (24)$$

to get the overall resolution.

4 Results

Table 3 is a guide to plots which show results of estimates of resolutions for the parameters in the design at this writing. In each figure, the upper left graph shows resolution contributions from the CDC, the upper right shows those from the FDC, and the lower left shows the combination of the CDC and FDC. The lower right contains a legend. In each of the upper plots (of the CDC and FDC alone), the contribution from position resolution is shown in yellow and that from multiple scattering is shown in blue. In addition, for the azimuthal resolution figures, there is a contribution from curvature error shown in magenta. CDC total resolution is displayed in red. This red curve is the same data for the CDC alone and in the combined. Likewise, the blue curve in the FDC alone graph and in the combined is the total resolution from the FDC and displays the same data in both cases. In addition, in each of the combined graphs at lower left there is a comparison with the results of HDGEANT⁵ for the same angle or momentum as appropriate.

abscissa ↓	ordinate →	$\delta p_t/p_t$	$\delta\theta$	$\delta\phi$
total momentum		Fig. 6	Fig. 7	Fig. 8
polar angle		Fig. 9	Fig. 10	Fig. 11

Table 3: Figures displaying resolution estimates as a function of momentum and polar angle.

5 Conclusions

The plots show reasonable agreement with the HDGEANT results. Agreement is generally at the 20% level, in some places better, in others as poor as a factor of 2.

One area where the simple model can break down is in the straight-line approximation for the trajectories for particles with very low transverse momentum. As a result predictions for extreme forward angles are suspect. We have already pointed out a problem with this approximation in estimating the contribution of curvature resolution to azimuthal angular resolution in Section 3.5. Also since the measurement are assumed to be equally spaced in both the FDC and the CDC, some of the features in resolution visible in the transition polar angle region between the two detectors is not reproduced; the real detector does not have a smooth loss of CDC hits and a smooth gain of FDC hits as the polar angle moves forward as does the model used in the estimates.

The most profitable use of these routines is probably not in predicting the absolute level of resolutions in the detector, but in predicting relative changes in resolution as detector parameters are changed. The former requires a more detailed modeling of the detector but also requires a greater effort whenever a new design is proposed. This resolution estimator (REZEST) is useful in exploring the parameter space during the optimization process.

A Some useful equations

This appendix contains some intermediate results in the calculation of the error on the slope in the case of equally spaced measurements.

⁵This is a full, hit-based Monte Carlo simulation of the detector with a least-squares fit of the trajectories.

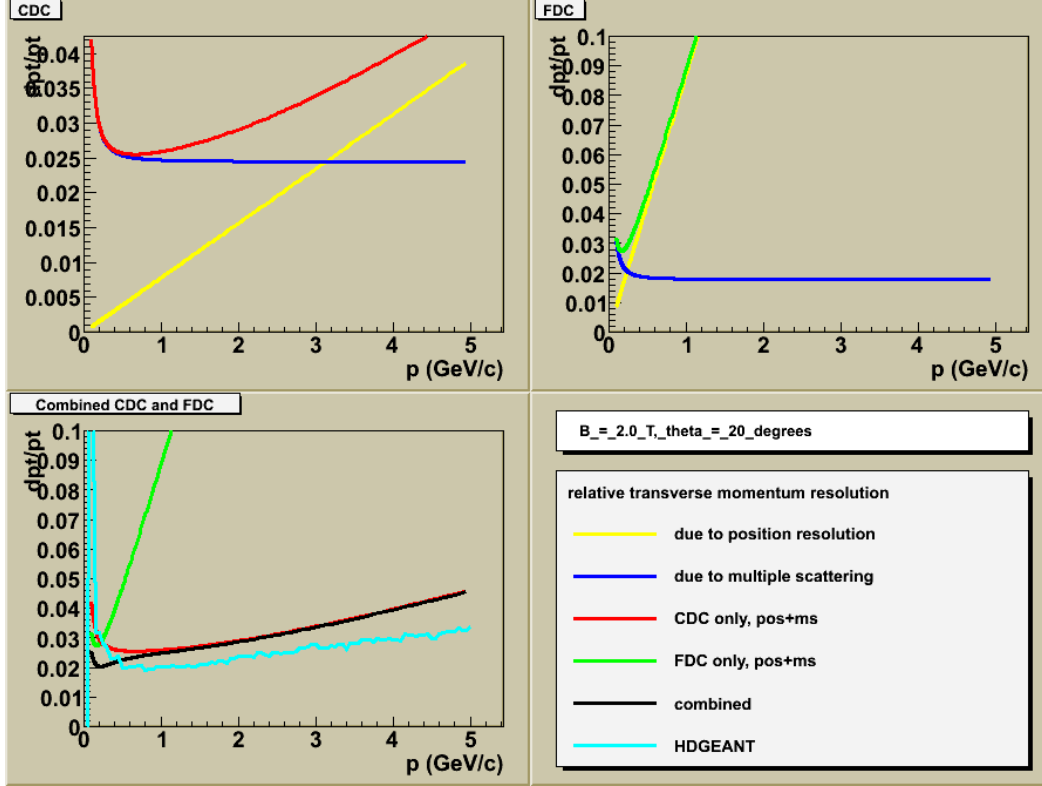


Figure 6: Estimates for resolution in relative transverse momentum as a function of total momentum at 20° for $B = 2.0$ T.

The well-known expressions

$$\sum_{i=1}^n i = \frac{n(n+1)}{2} \quad (25)$$

and

$$\sum_{i=1}^n i^2 = \frac{n(n+1)(2n+1)}{6} \quad (26)$$

allow us to obtain the following results for equally space measurements:

$$\sum x_i = \frac{nL}{2} \quad (27)$$

$$\sum x_i^2 = \frac{L^2 n(2n-1)}{6(n-1)} \quad (28)$$

and for the parameter in the straight-line-fit error expressions we get

$$\Delta' = \frac{L^2 n^2 (n+1)}{12(n-1)}. \quad (29)$$

References

- [1] Philip R. Bevington and D. Keith Robinson. *Data Reduction and Error Analysis for the Physical Sciences*. McGraw-Hill, New York, 2nd edition, 1992.
- [2] W. M. Yao et al. Review of particle physics. *J. Phys.*, G33:1–1232, 2006.

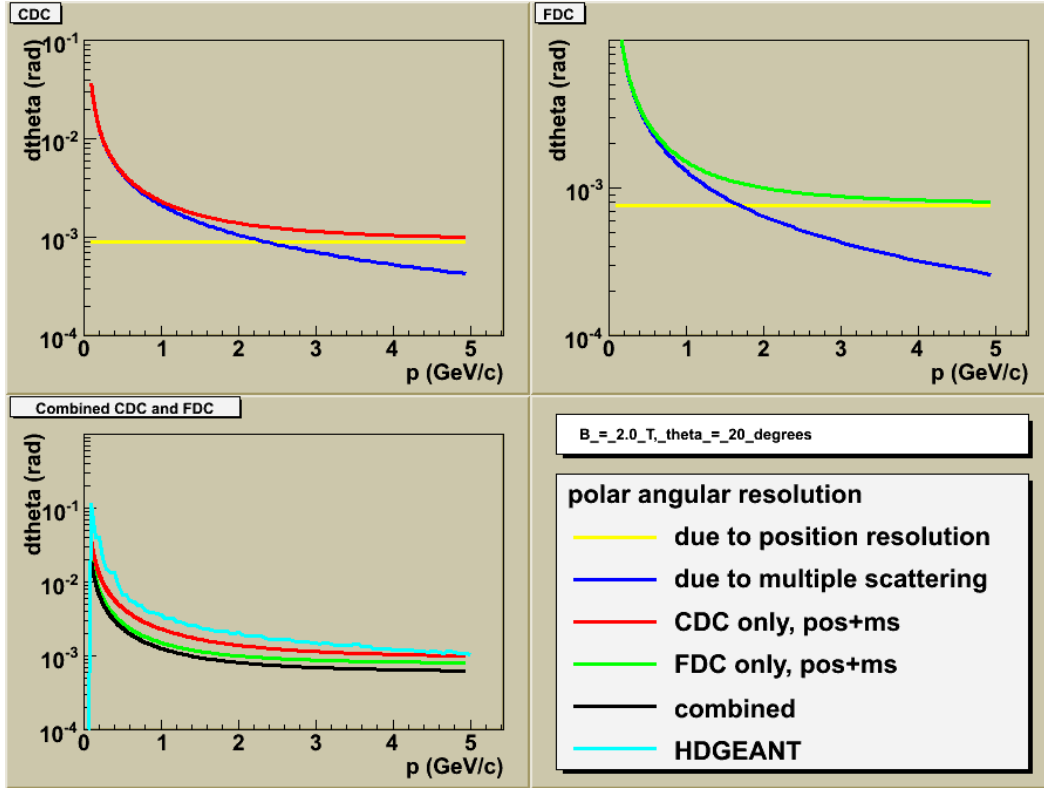


Figure 7: Estimates for resolution in polar angle as a function of total momentum at 20° for $B = 2.0$ T.

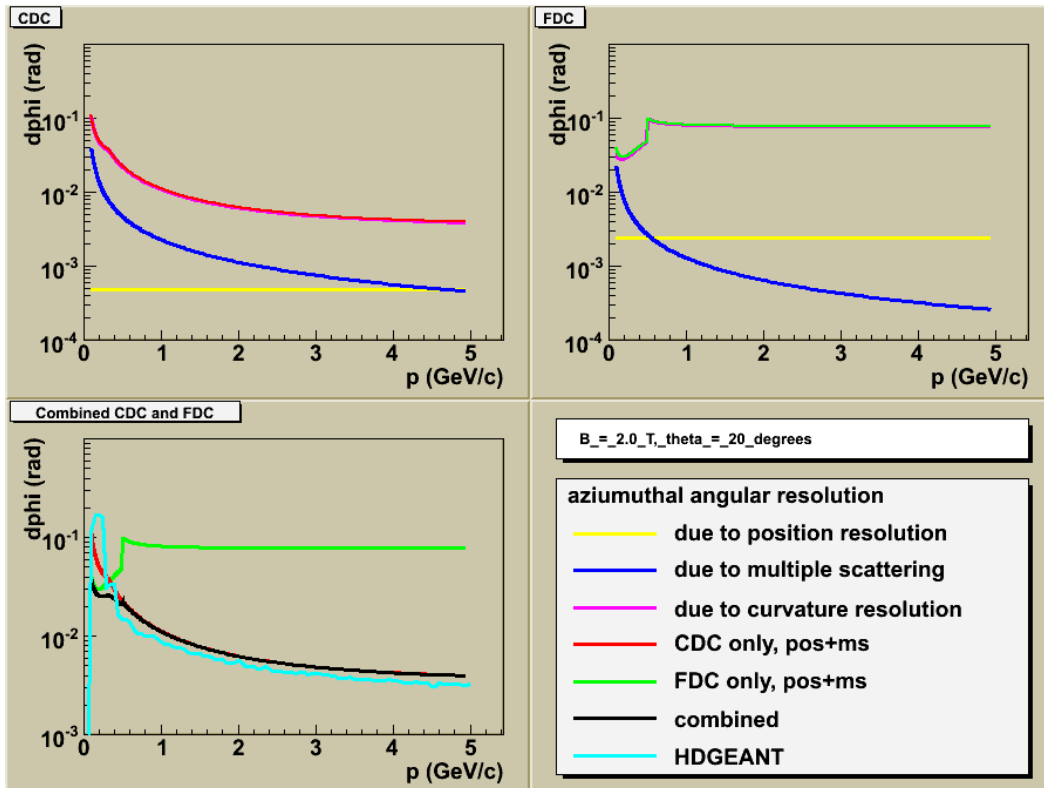


Figure 8: Estimates for resolution in azimuthal angle as a function of total momentum at 20° for $B = 2.0$ T.

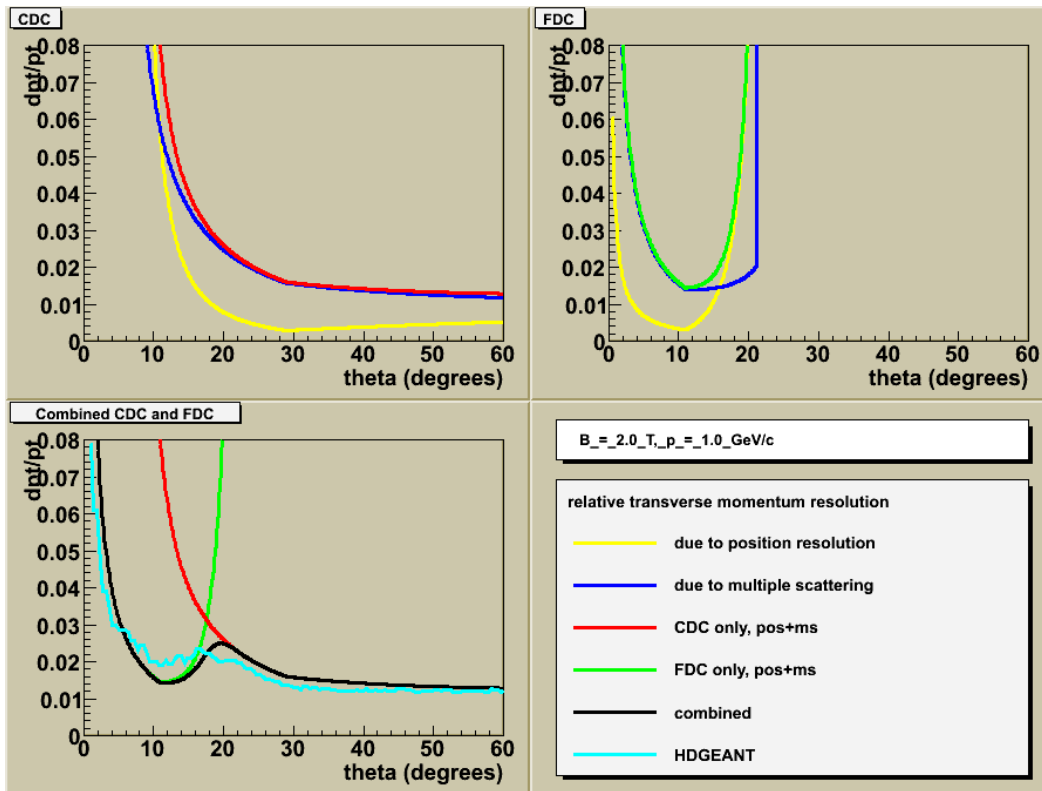


Figure 9: Estimates for resolution in relative transverse momentum as a function of polar angle at $p = 1.0$ GeV/c for $B = 2.0$ T.

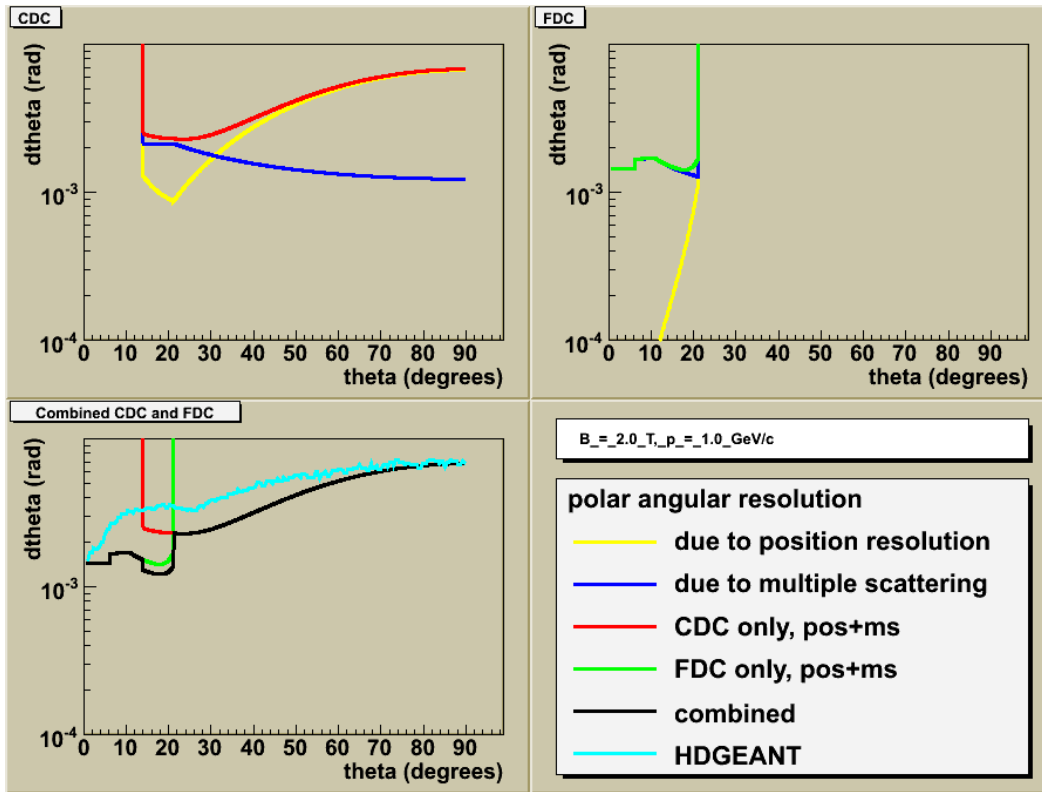


Figure 10: Estimates for resolution in polar angle as a function of polar angle at $p = 1.0 \text{ GeV}/c$ for $B = 2.0 \text{ T}$.

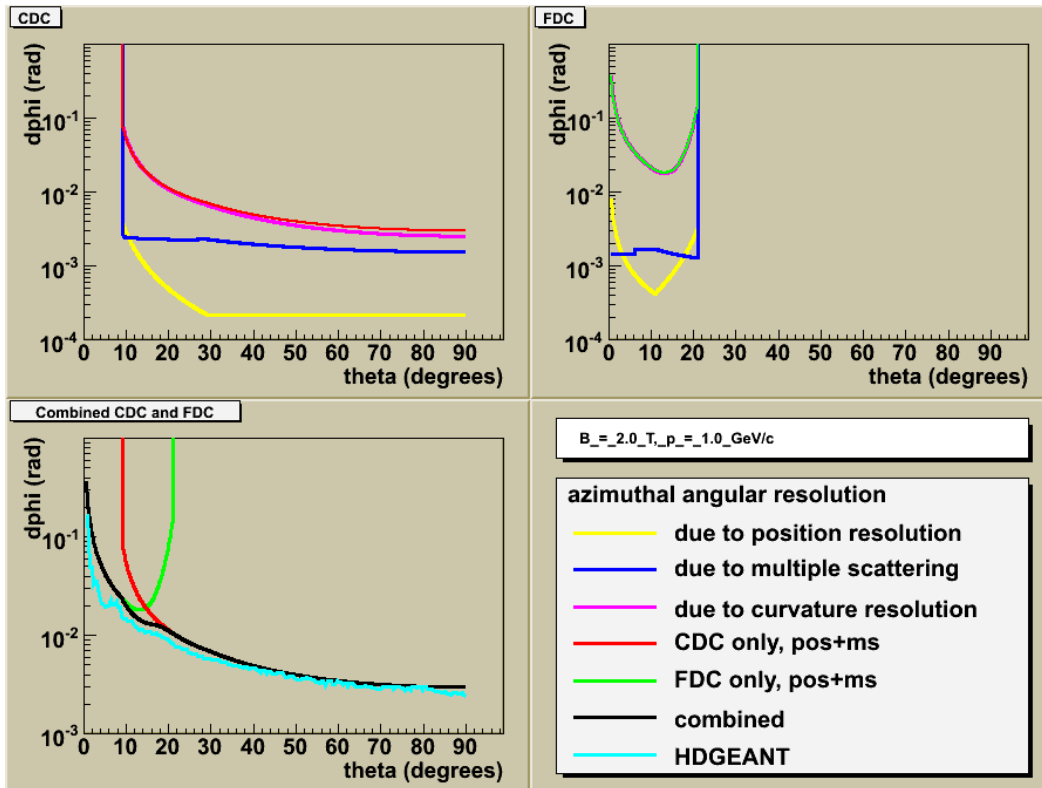


Figure 11: Estimates for resolution in azimuthal angle as a function of polar angle at $p = 1.0$ GeV/ c for $B = 2.0$ T.